

Transient modeling of slag foaming using computer fluid dynamics simulations

Eder Trejo^{a,b}, Lidong Teng^a, Alejandro Montesinos^b, Seshadri Seetharaman^a

^aDepartment of Materials Science and Engineering, Division of Materials Process Science, Royal Institute of Technology, Brinellvägen 23, Stockholm 10044, Sweden.

^bInstituto Tecnológico y de Estudios Superiores de Monterrey, School of Engineering and Information Technologies, Ave. Eugenio Garza Sada 2501, Monterrey 64849, México.

Abstract: During operation of the EAF (Electric Arc Furnace) it is important to have a good foaming practice in order to maintain the arc covered with foaming slag. A lot of efforts have been made to develop a mathematical model to describe and better understand the phenomena. In this work, a slag model based in computer fluid dynamics (CFD) and bubble balance is presented. The advantage of this approach is its flexibility to be applied in several steel processes and its possibility to be run in a real time simulation. The main parameters of the model were estimated based in laboratory scale experiments and the simulations showed a good agreement with the experimental results.

Keywords: Electric arc furnace, Slag foaming, Computer fluid dynamics, Transient model

1. Introduction

The current computational tools, specifically computer fluid dynamics (CFD) can handle complex relationships which may involve more variables and their effects on slag foaming and can be suitable to develop more flexible models to be applicable in various operating conditions. In the present paper a CFD dynamic simulation for slag foaming based on physical and chemical equations that describe the process is presented; model predictions are in good agreement with experimental data obtained. With this approach it will be possible to increase the flexibility of the current models and will give information about the correct parameters used to achieve an accurate dynamic simulation of the slag foaming, which is essential to maintain the arc covered in order to obtain significant savings in energy, refractory and electrodes consumption within the EAF.

2. Slag foaming models

Actual models [1,7] require very specific experiments to estimate its parameters, most of them have taken data from various sources, without considering that the experimental conditions (such as dimensions of the container in which the foaming takes place) may vary significantly the results. The parameters shown in the models only work in a narrow range of operating conditions and require very precise experimental data in order to extend its application to industrial level.

A stronger disadvantage of the actual models is that they perform the calculation of foam in steady state, which, according to experiments conducted by Kapilashrami et al.[8] leads to considerable deviations comparing experimental results in transient state against the application of foaming models in steady state. According to Kapilashrami et al.[8] traditional theories are not valid for foaming under dynamic (transient) conditions. In the same sense, Stadler et al.[9] states that there is still little understanding of the phenomenon of slag foaming and emphasized the need for more experimental data to contribute to the development of knowledge in the area.

3. Model development

In order to develop a general model of slag foaming, it is necessary to consider the fundamental equations involved in the phenomena which describe the fluid dynamics of the liquid metal where the gas injection take place; the bubble size distribution in the foam is also considered in the present model. The foaming model consist of three main parts: fluid dynamics estimation in the liquid metal, bubble population balance in the liquid metal and foam height estimation in the liquid slag. The velocity field of the liquid metal is estimated by solving the Navier-Stokes equations using the finite differences technique. Then, the gas phase in the liquid metal is estimated as a volume fraction in the continuous phase (liquid metal). The gas fraction at the metal surface is then used to define a bubble size and distribution to estimate the foam height in the liquid slag.

3.1 Equations solution

In order to solve the equation, an approximate finite element algorithm based in the method used by [10] and [11] was adopted. First, the velocity field was solved in a "velocity step", then, a "volume fraction step" was performed to compute the volume fraction of gas in the liquid metal; the last is the "foam step" which solves the bubble distribution in the liquid slag to estimate the foam height.

3.1.1 Velocity step

The Navier-Stokes equations for incompressible flow and constant density were adopted to solve the velocity field in the liquid metal considering two-dimensional flow.

$$\frac{\partial}{\partial t} \mathbf{v} + \mathbf{v} \cdot \nabla \mathbf{v} = -\frac{1}{\rho} \nabla p + \mu \nabla^2 \mathbf{v} + \mathbf{F} \quad (1)$$

The approximate solution of the equation is performed by defining an initial velocity field and applying successive modification steps to include the boundary conditions, molecular transport and advective transport. In case of the momentum equation, an additional step called projection is performed in order to make the solution mass conservative. According to this, the algorithm was organized in boundary set, diffusion step, projection step, advective step and projection step once again.

3.1.1.1 Boundary set

In case of the velocity field, a non-slip condition for the walls and metal slag interphase was applied. For the injection points, a uniform velocity was set in every time step:

$$v_{x \ i,j} = v_{0x \ n} \quad (2)$$

$$v_{y \ i,j} = v_{0y \ n} \quad (3)$$

where i,j are the relative coordinates (referred to the number of nodes in the mesh) of the injection point n , and v_0 is the velocity magnitude for each of the velocity components. The force additions were added in this step, using the volume fraction to estimate the buoyant forces in the liquid metal.

$$F_{y_{i,j}}^{t+\Delta t} = g \frac{\rho_{gas}}{\rho_{st}} (\rho_{st} - \rho_{\alpha_{i,j}}^t) \quad (4)$$

were

$$\rho_{\alpha_{i,j}}^t = \rho_{gas} \varphi + \rho_{st} (1 - \varphi) \quad (5)$$

For the volume fraction estimation, the boundary conditions were set as unity at the injection points for each time step.

$$\varphi_{k_{i,j}}^{t+\Delta t} = 1 \quad (6)$$

3.1.1.2 Diffusive step

For the diffusive step, the Poisson equation was solved numerically using the formula

$$x_{i,j}^{t+\Delta t} = \frac{x_{i-1,j}^t + x_{i+1,j}^t + x_{i,j-1}^t + x_{i,j+1}^t + \gamma b_{i,j}}{\beta} \quad (7)$$

where x represents p, v_x, v_y , or ρ_{α} . When $x = p$ $\gamma = -(\Delta x)^2$, $b = \nabla \cdot \mathbf{v}$ and $\beta = 4$. For the viscous diffusion equation $x = b$ and represents the components of \mathbf{v} , $\gamma = (\Delta x)^2 / \nu N_x \Delta t$, and $\beta = 4 + \gamma$.

3.1.1.3 Advective step

The advective step represents the transport of any property q caused by the velocity field. The arbitrary property q can represent \mathbf{v}, n_d or any other property carried by the fluid; the formula used to estimate the advection is

$$q_s^{t+\Delta t} = q_{s-\Delta t \mathbf{v}_{s,t}}^t \quad (8)$$

where s is the position of the particle at time $t + \Delta t$ and $s - \Delta t \mathbf{v}_{s,t}$ is the position of the particle at time t . This method considers the property as a particle, then the trajectory of the "particle" from each grid is traced back in time to its former position to the starting grid cell.

3.1.1.4 Projection step

The velocity field estimated with the previous steps will have a non-zero divergence; but in order to satisfy the continuity equation, it is necessary to have a zero divergence velocity field. The Helmholtz-Hodge decomposition theorem permits to correct the velocity field to maintain the mass conservation.

$$\mathbf{v} = \mathbf{w} - \nabla p \quad (9)$$

where \mathbf{w} is the velocity field with nonzero divergence and \mathbf{v} is the corrected divergence-free velocity field.

3.1.2 Volume fraction step

To estimate the transport of the gas phase in the liquid metal, a simplified case of the general equation for continuity of species was applied. In this equation, the property transported by the velocity field and molecular diffusion was the volume fraction

$$\frac{\partial}{\partial t} \varphi + \mathbf{v} \cdot \nabla \varphi = D_g c \nabla^2 \varphi \quad (10)$$

where D_{g_c} represents the solubility of the dispersed phase, g in the continuous phase c . In our model, it is assumed that solubility of the gas bubbles in the metal is negligible, so it is possible to eliminate the diffusive term to get

$$\frac{\partial}{\partial t} \varphi + \mathbf{v} \cdot \nabla \varphi = 0 \quad (11)$$

The solution of this equation gives the volume fraction distribution in the liquid metal bath, which can be used later in the Foam step to estimate the slag foaming height.

3.1.3 Foam step

The Foam step considers each individual bubble as a sphere surrounded by a thin layer of liquid slag. The bubbles can be of any number of different sizes; however, in this model only 10 sizes are considered as the addition of more sizes does not give an important impact on the model results. The bubble sizes are distributed between a minimum and a maximum stable diameter with an exponential factor. The minimum stable diameter was estimated with an equation proposed by Hesketh et al.[12] using the maximum velocity in the liquid metal.

$$d_s = \left(\frac{W_{e_{crit}}}{2} \right)^{0.6} \left[\frac{\sigma^{0.6}}{(\rho_c^2 \rho_d)^{0.2}} \right] \varepsilon^{-0.4} \quad (12)$$

The maximum diameter is set based in the actual process. The distribution of bubbles of each size is estimated proportionally to the gas volume fraction in the liquid metal surface and the number of bubbles of each size is estimated with the bubble volume and the gas volume leaving the liquid metal bath V_{out} in each time step.

$$V_{out}^t = V_{in}^t - \int \varphi^t dV \quad (13)$$

Once the number of bubbles of each size are estimated N_j , a bubble balance is performed. The small bubbles can join to produce a bigger one, however, big bubbles can not split in small ones. In this model, the bubble coalescence (joining of bubbles) can be only binary.

$$N_j^{t+\Delta t} = N_j^t + N_{j_{in}}^t - \sum_{i=j}^{10} \uparrow k_{j,i} N_j^t \cdot N_i^t + \sum_{i=1}^j \uparrow Y_{j,i} k_{j,i} N_j^t \cdot N_i^t \cdot m \quad (14)$$

Where $k_{j,i}$ is a triangular matrix containing the kinetics constants which depends of the probability of the coalescence of bubbles with certain size and a temporal parameter which considers the time necessary for the bubble coalescence. Similarly $Y_{j,i}$ is a square matrix with the volume proportion between the different bubble sizes and zeros in the main diagonal. In order to estimate the values of $k_{j,i}$ a uniform probability distribution was used for each bubble size and a linear behavior between a minimum (kd_{min}) and maximum (kd_{max}) coalescence factor was adopted. The values of these two parameters were estimated based in experimental results of argon injection in liquid slag. In order to avoid an overestimation of slag height by bubble production, a limitation based on the slag mass available m was set for the bubble production. The variable m has a value of unity when there is liquid slag available to produce new bubbles, and has a value of zero when no liquid slag is available. The total slag mass of the bubbles was estimated with a wall thickness. For simplicity, a linear relation which depends of the viscosity and surface tension was assumed.

$$\delta = \frac{k_t \sigma}{\mu} \quad (15)$$

where k_t is a model parameter to be found experimentally.

4 Results and discussion

The algorithm was programmed and run for different cases. It showed a good stability allowing fluid simulations in real time and high flexibility to change the positions of injection points and its velocity magnitude. The implementation of the model for a 6.5 meter-EAF with two injection points is shown in the Figure 1.

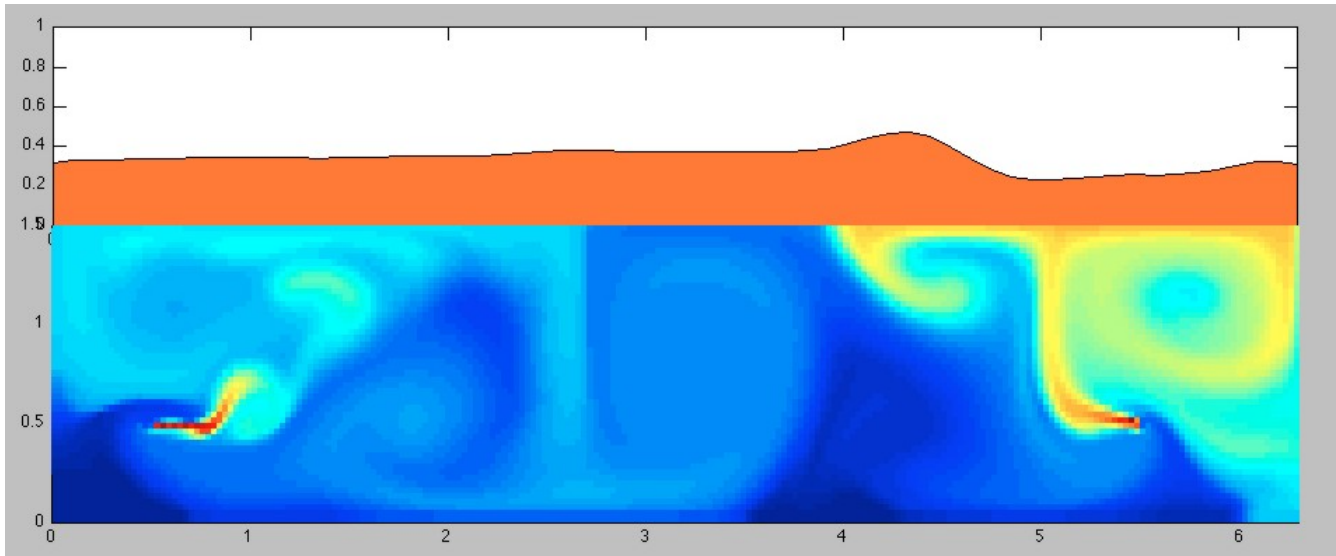


Figure 1: Volume fraction field and slag foaming height simulation in an EAF.

In order to estimate the model parameters as time step, maximum and minimum coalescence constants, a small scale simulation was performed and compared with experimental results. The experiment performed consisted on injecting argon in liquid slag at 1680 °C. The slag was contained in a Boron nitride crucible and the argon was injected at 20, 30 and 40 cm^3/min . The experiment were carried out in a laboratory scale furnace. The values of the parameters calculated for the model are shown on Table 1.

Table 1: Parameter values used in the model.

Parameter	Value
Courant number	1-10
kd_{max}	0.5
kd_{min}	0.02
Bubble distribution factor	25
k_t	1250

The model can manage multiple injection points and allowed to change the position and velocity magnitude of the gas injected. The predicted foam presents spacial and temporal fluctuations which previous models were not able to manage [8]. The simulation velocity depends of the velocity magnitude used as it is an important parameter in the Courant number estimation. For velocities lower than 10 m/s, the simulation can be performed in real time using conventional computers.

5 Conclusions

In the present paper a CFD dynamic simulation for slag foaming based on physical equations that describe the process is presented; the model flexibility allows its implementation in different slag foaming processes and its application can be extended to other cases like flotation cells.

With this approach, it is possible to increase the flexibility of the current models and will give information about the correct parameters used to achieve an accurate dynamic simulation of the slag foaming, which is essential to maintain the arc covered in order to obtain significant savings in energy, refractory and electrodes consumption within the EAF. The main parameters used in the model were estimated based in experimental results of slag foaming at laboratory scale. The model shows good agreement with the experimental data.

Acknowledgements

We wish thank Ternium and Tenaris-Tamsa companies, with whose funds have made possible this research. We also appreciate the laboratory facilities provided by the Division of Materials Process Science at KTH and the support provided by ITESM Campus Monterrey.

Nomenclature

\mathbf{v}	Velocity vector
v	Velocity component
g	Gravitational constant
φ	Volume fraction
h	Slag height
N_j	Number of bubbles of size j
$\mathcal{D}_{g\ c}$	Diffusivity
ρ	Density
μ	Viscosity of slag
σ	Surface tension of slag
F	Force field
\mathbf{k}	Coalescence constant matrix
kd_{max}	Maximum coalescence constant
kd_{min}	Minimum coalescence constant
k_t	Thickness constant
m	Factor to determine the availability of liquid slag
δ	Wall thickness
V	Wall thickness

We_{crit}	Gas volume
Y	Critic Weber number
ε	Yield constant matrix
	Turbulent energy

References

- [1] Ito K, Fruehan R. Study on the foaming of CaO-SiO₂-FeO slags: Part II. Dimensional analysis and foaming in iron and steelmaking processes. *Metallurgical and Materials Transactions B*. 1989;20(4):515-21.
- [2] Zhang Y, Fruehan RJ. Effect of the bubble-size and chemical-reactions on slag foaming. *Metallurgical and Materials Transactions B-Process Metallurgy and Materials Processing Science*. 1995;26(4):803-12.
- [3] Ghag SS, Hayes PC, Lee HG. Model development of slag foaming. *Isij International*. 1998;38(11):1208-15.
- [4] Wu K, Qian W, Chu SJ, Niu Q, Luo HW. Behavior of slag foaming caused by blowing gas in molten slags. *Isij International*. 2000;40(10):954-7.
- [5] Ghag SS, Hayes PC, Lee HG. The prediction of gas residence times in foaming CaO-SiO₂-FeO slags. *Isij International*. 1998;38(11):1216-24.
- [6] Pilon L, Fedorov AG, Viskanta R. Steady-state thickness of liquid-gas foams. *Journal of Colloid and Interface Science*. 2001;242(2):425-36.
- [7] Matsuura H, Fruehan RJ. Slag Foaming in an Electric Arc Furnace. *Isij International*. 2009;49(10):1530-5.
- [8] Kapilashrami A, Gornerup M, Lahiri AK, Seetharaman S. Foaming of slags under dynamic conditions. *Metallurgical and Materials Transactions B-Process Metallurgy and Materials Processing Science*. 2006;37(1):109-17.
- [9] Stadler SAC, Eksteen JJ, Aldrich C. An experimental investigation of foaming in acidic, high FeO slags. *Minerals Engineering*. 2007;20:1121-8.
- [10] Stam, J. 1999. "Stable Fluids." In *Proceedings of SIGGRAPH 1999*.
- [11] Randima Fernando. 2004. *GPU Gems: Programming Techniques, Tips and Tricks for Real-Time Graphics*. Pearson Higher Education.
- [12] Hesketh R, Etchells A, Russell T. Bubble breakage in pipeline flow. *Chemical Engineering Science*. 1991;46(1):1-9.